


 Cite this: *RSC Adv.*, 2022, 12, 16141

Preparation of an eco-friendly antibacterial agent for food packaging containing *Houttuynia cordata* Thunb. extract

 Peifu Kong,^a Junichi Peter Abe,^b Akiko Nakagawa-izumi,^b Mikio Kajiyama^b and Toshiharu Enomae^{*b}

This study aims to develop an antibacterial agent that can be used for food packaging. Essential oils of *Houttuynia cordata* Thunb., a well-known medical herb, were extracted by two methods: multi-solvent consecutive extraction method and single ethanol extraction with a pre-heating method. Consequently, the extract obtained by the single ethanol extraction with a pre-heating method was more satisfactory from the operational and economic aspects. Afterwards, one of the encapsulation techniques: co-precipitation method using β -cyclodextrins as wall materials, was applied to form capsules for the protection of the obtained extract. After the capsule synthesis, the results of scanning electron micrographs and X-ray diffraction showed β -cyclodextrin crystallites in the form of thinner plates became oriented upon co-precipitation. Combining the results of Fourier transform-infrared spectra and an antibacterial assay using *Bacillus subtilis* as an object microorganism, the extract was confirmed to be successfully encapsulated within hollow cavities of β -cyclodextrins. A significant inhibitory activity on the growth and breeding of *Bacillus subtilis* was observed after the addition of fabricated capsules, which suggests the capsules containing the *Houttuynia cordata* Thunb. extract can be used as eco-friendly antibacterial agents for food packaging.

 Received 4th April 2022
 Accepted 19th May 2022

DOI: 10.1039/d2ra02178a

rsc.li/rsc-advances

1 Introduction

Packaging is forming a more and more inalienable part of our daily life. However, in the field of food packaging, microorganism contamination gives rise to the spread of disease and reduces the shelf life of food.¹ Along with the sudden outbreak of the COVID-19 pandemic being life-threatening across the globe, increasing cases of food contact infection have accelerated the demand for antimicrobial packaging materials.

To date, there has been considerable interest in developing biodegradable antimicrobial food packaging materials because of the pressure of environmental concerns stemming from the traditional plastic materials made from petroleum which are non-biodegradable and non-renewable. Nanoparticles of gold, silver and zinc oxide as nanofillers have been successfully exploited with biodegradable polymers (*e.g.*, chitosan, cellulose, gelatin and alginate) to obtain antimicrobial composite films for food packaging.^{2–6} Wu *et al.*⁷ firstly reported that LAPONITE[®] immobilized silver nanoparticles can be synthesized with quaternized chitosan and the prepared silver nanoparticles-chitosan film was successfully applied for keeping litchis

fresh. Tsai *et al.*⁸ revealed that the gold–silver nanoparticles could be successfully immobilized onto a cellulose film by heat treatment and an antibacterial activity of the gold–silver nanoparticles-cellulose film against *Escherichia coli* was presented. In another research reported by Kanmani *et al.*,⁹ active nanocomposite films were prepared by blending aqueous solutions of gelatin with different concentrations of silver nanoparticles using a solvent casting method and exhibited a strong antibacterial activity against some food-borne pathogens. However, there is a serious consumer concern about the risks posed by the introduction of metal nanoparticles into food packaging, which could place restrictions on their benefits as the metal nanoparticles can be neutralized on contact with food or diffuse rapidly from the surface of packaging into the food mass. Moreover, these metal nanoparticles may enter the human body through food, triggering certain physiological reactions.¹⁰ With the consideration of this security concern, the research group of Motelica *et al.*^{11–13} developed antimicrobial composite films containing a low concentration level of metal nanoparticles which were mixed with essential oils (EOs) previously. Due to a synergy of metal nanoparticles and EOs, the fabricated composite films exhibited an excellent antimicrobial coverage, and presented great UV light barrier property and low water vapor permeability. Besides, their fabricated films have been successfully used for the preservation of cheese and grapes. Nevertheless, the addition of a low concentration of

^aDegree Programs in Life and Earth Sciences, University of Tsukuba, Tsukuba, Ibaraki, 305-8572, Japan. E-mail: enomae.toshiharu.fw@u.tsukuba.ac.jp

^bFaculty of Life and Environmental Sciences, University of Tsukuba, Tsukuba, Ibaraki, 305-8572, Japan



metal nanoparticles is still remaining controversial due to their possible toxicity and potential hazards.^{13,14}

A prospective alternative is produced from substances totally isolated from botanical sources such as EOs. EOs are volatile compounds from aromatic plants with a range of phyto-pharmacological properties, including antimicrobial, anti-allergic, antitumor, antioxidative, and so forth. Extensive attention has been paid to EOs since they are natural products and have been considered as Generally Recognized as Safe food additives by the Food and Drug Administration.^{15,16} Since time immemorial, EOs have been utilized for aromatic and flavouring purposes and also in traditional medicines in Asia.^{17–19} Nevertheless, high volatility, high heat sensitivity, and easy oxidation impede their performances, and these defects may be sufficient to alter the quality of their applications.^{20,21}

Encapsulation is required to prevent those performance reductions mentioned above and is crucial from a scientific, industrial and economical point of view,^{22,23} and has attracted a great deal of interest such as its current applications in medicine, catalysis, cosmetics, and foods. In the biomedical field, capsules prepared from biodegradable polymers as wall materials have been frequently utilized to drugs for controlled and sustained release.^{21,24–28} This technique could be generally divided into three categories, which are physical methods including co-precipitation and spray drying, physicochemical methods including coacervation and sol–gel encapsulation, and chemical methods such as *in situ* polymerization and the use of liposomes.^{29–31} Table 1 shows some applications of various encapsulation methods for EOs. Among them, the co-precipitation method using β -cyclodextrins (β -CD) has been generally utilized as β -CD have hydrophilic outer surfaces and hydrophobic hollow cavities which can embed EOs by use of their similar physical property.

Houttuynia cordata Thunb. referred-to as “HC” hereafter, a perennial herb, is a plant of the Saururaceae family predominantly distributed in Asia. This plant, universally known across Japan as “Dokudami”, has been used as a traditional remedy for the treatment of various diseases or symptoms in local areas of

Japan and China.^{32–34} Japanese Pharmacopoeia guidebook in the 18th edition (2021) lists it and describes that the aerial parts of HC can ameliorate the symptoms of constipation and chronic skin diseases, and its decoction can facilitate diuretic and anti-inflammatory effects.³⁵ Das *et al.*³⁶ reported the bioactive phyto-compounds from HC can be applied as potential inhibitors for three main replication proteins of SARS-CoV-2, which control the replication process of COVID-19 infection. Furthermore, the traditional Chinese medicine “Lianhua Qingwen” including HC has been proved to be an effective therapy for the treatment of mild COVID-19 patients and employed since year 2020.³⁷ Some reports have revealed that HC contains sundry active constituents such as EOs, flavonoids, alkaloids, organic and fatty acids, sterols and microelements, which possess diverse pharmacological activities including diuretic, antibacterial, antiviral, antitumor, anti-inflammatory, antioxidative, anti-diabetic, anti-allergic, and anti-mutagenic effects.^{38,39} A large number of reports have confirmed that the antimicrobial effect of HC primarily comes from EOs which show a significant inhibitory effect on SARS coronavirus, HSV, *Bacillus cereus*, *Bacillus subtilis* (*B. subtilis*), *Staphylococcus aureus*, *Vibrio parahaemolyticus*, *Penicillium*, *Aspergillus niger*, and so on.^{33,40} The conventional process to obtain EOs from aromatic plants is steam distillation, which is time-consuming and requires plenty of samples.³³ Herein, organic solvent extraction as a feasible alternative was applied, and *B. subtilis* was chosen as the object microorganism to evaluate the antibacterial activity of its extract.

The aim of this research is to develop a capsule of EOs extracted from HC as an antibacterial agent for food packaging. The study is composed of the following three phases: (1) EOs extraction from HC using the two methods: multi-solvent consecutive extraction (MCE) method and single ethanol extraction with a pre-heating (SEEP) method, (2) synthesis of capsules by co-precipitation using β -CD and (3) characterization and antibacterial assessment of the fabricated capsules.

Table 1 Examples of encapsulation methods for EOs

Author	Core material	Wall material	Preparation method	Capsule diameter (μm)	Application
Arana-Sánchez <i>et al.</i> ⁴¹	Oregano oil	β -CD	Co-precipitation	<30	Antimicrobial and antioxidant agents
Kfoury <i>et al.</i> ⁴²	Nine selected EOs	Six kinds of cyclodextrin	Co-precipitation	No data	Radical scavenging efficacy
Karaaslan <i>et al.</i> ⁴³	Pepper seed oil	Gum arabic and maltodextrin	Spray drying	0.5–80	Antimicrobial and peroxidative stability
Hsieh <i>et al.</i> ⁴⁴	Citronella oil	Chitosan	Simple coacervation	10–250	Controlled release
K. Rutz <i>et al.</i> ⁴⁵	Palm oil	Chitosan and xanthan; chitosan and pectin	Complex coacervation	<5	Controlled release
Songkro <i>et al.</i> ⁴⁶	Citronella oil	Gelatin and gum Arabic	Complex coacervation	<8	Mosquito repellents
Vega <i>et al.</i> ⁴⁷	Nine selected EOs	Hybrid organic-inorganic silica	Sol-gel	Not specified	Antibacterial agents
Lee <i>et al.</i> ⁴⁸	Floral oil	Melamine and formalin	<i>In situ</i> polymerization	12–15	Not specified
Sebaaly <i>et al.</i> ⁴⁹	Clove oil	Soybean	Liposome	200–320	Stability improvement of eugenol



2 Experimental

2.1. Plant materials and EOs extraction

HC was picked in the campus of Univ. of Tsukuba around September and stored in a freezer (approx. $-20\text{ }^{\circ}\text{C}$). The storage time of all HC used in this study was within one month.

2.1.1. MCE method. The ingredients of HC have an extremely wide variety, including EOs, flavonoids, alkaloids, organic acids, amino acids, proteins, vitamins, trace metal elements and some other greases.^{33,34} In this method, three solvents: hexane, ethyl ether and ethanol in order of increasing polarity were used. It is assumed that the ingredients of HC can be divided into three groups *via* using the three solvents: firstly, greases and some proteins can be removed primarily with hexane with the lowest polarity among the three solvents; secondarily, active phytochemicals of EOs such as terpenes containing a certain amount of hydroxyl or carboxyl groups resemble ethyl ether in polarity, being prone to be with an affinity for it, can be removed with ethyl ether; thirdly, the remaining constituents such as alkaloids and organic acids are supposed to be separated out in ethanol. The experimental details were as follows: a total of 50 g (± 0.5 g) of frozen HC was added to 200 mL of hexane (guaranteed reagent, FUJIFILM Wako Chemicals, Japan) in a conical flask and extracted continuously at $45\text{ }^{\circ}\text{C}$ on a hot plate for 2 h. Afterwards, the filtrate was collected *via* a suction filtration process (AS-01, AS ONE Corporation, Japan) with a filter paper with a pore diameter of $1\text{ }\mu\text{m}$ (No. 4, Kiriya glass. Co., Japan, applied for all filtration processes hereafter). The residue on the filter was further extracted with 200 mL of ethyl ether (guaranteed reagent, FUJIFILM Wako Chemicals, Japan) at $45\text{ }^{\circ}\text{C}$ for 2 h and then the filtrate was collected *via* the suction filtration. Similarly, the residue on the filter was again further extracted with 200 mL of 99.5% ethanol (guaranteed reagent, FUJIFILM Wako Chemicals, Japan) at $45\text{ }^{\circ}\text{C}$ for 2 h and then the filtrate was collected *via* the suction filtration. The three filtrates at the three stages were concentrated to approx. 20 mL to obtain hexane extract of HC (referred-to as “heHC(MCE)” hereafter), ethyl ether extract of HC (referred-to as “eeeHC(MCE)” hereafter) and ethanol extract of HC (referred-to as “eeHC(MCE)” hereafter) using a rotary evaporator (N-1000, Tokyo Rikakikai Co., Ltd., Japan) and stored in a sealed conical flask at room temperature before subsequent antibacterial evaluation.

2.1.2. SEEP method. A survey in Kochi Prefecture, Japan, on how to use HC as a traditional treatment was performed and the result showed that 96% of the local people surveyed believed that the fresh leaves of HC, subjected to a pre-heating process, were extremely effective as a remedy for skin diseases.⁵⁰ Therefore, based on this empirical approach, a SEEP method was carried out to obtain EOs. In this method, a total of 10 g (± 0.1 g) of frozen HC wrapped in aluminium foil was heated in an electromagnetic cooker (set to the fourth level among six output levels, 2 kW at maximum) for 2 min and a paste-like HC product was obtained. The HC paste *via* this heating process is referred to as “HCP”. After that, an ethanol extract of HCP, referred-to as “eeHCP(SEEP)”, was prepared in the following

way.⁵⁰ The HCP was put into 5 mL of 99.5% ethanol, and extracted using a vortex mixer (HS120214, Heathrow Scientific, LLC, USA) at 3000 rpm for 10 min and then centrifuged at 1400 g for 5 min. After centrifugation, the supernatant which is considered as eeHCP(SEEP) above the sedimented HCP was collected *via* the suction filtration and stored in a sealed glass vial at $23\text{ }^{\circ}\text{C}$ before antibacterial evaluation. As a control, ethanol extract of HC, referred-to as “eeHC(SEEP)”, without the step of pre-heating in an electromagnetic cooker was prepared in the same condition as mentioned above.

2.2. Identification of EOs extracted from HC

As discussed in Section 3.1 of the “Result and Discussion” part later, based on an antibacterial evaluation for all obtained extracts by the two extraction methods, the eeHCP(SEEP) was most satisfactory from the operational and economic aspects. Therefore, only eeHCP(SEEP) was used for the identification of EOs and subsequent encapsulation procedure and characterization.

The identification of EOs in eeHCP(SEEP) was conducted using a gas chromatography-mass spectrometry (GC-MS). Here, the eeHC(SEEP) was set as a control. The condition details were as follows: injecting $2\text{ }\mu\text{L}$ of an eeHCP(SEEP) or eeHC(SEEP) solution into a GC-MS-QP2010Plus (Shimadzu, Japan) with a Rtx-5MS column ($30\text{ m} \times 0.25\text{ }\mu\text{m}$, $0.25\text{ }\mu\text{m}$ in film thickness). The oven temperature of GC was programmed described by Pan *et al.*³² with a few modifications: kept at $60\text{ }^{\circ}\text{C}$ for 2 min, then increased to $125\text{ }^{\circ}\text{C}$ at a rate of $10\text{ }^{\circ}\text{C min}^{-1}$ and maintained for 5 min, to $165\text{ }^{\circ}\text{C}$ at $10\text{ }^{\circ}\text{C min}^{-1}$ and held for 10 min, to $185\text{ }^{\circ}\text{C}$ at $2\text{ }^{\circ}\text{C min}^{-1}$, and finally to $240\text{ }^{\circ}\text{C}$ at $10\text{ }^{\circ}\text{C min}^{-1}$ and maintained for 10 min. The injector temperature was $260\text{ }^{\circ}\text{C}$ and the flow rate of carrier helium gas was 1.5 mL min^{-1} with a split ratio of 10 : 1. The mass spectrometer was operated in the electron impact (EI) mode at 70 eV and mass spectra were acquired using a scan mode with a mass scan range of 50–650 *m/z*. The temperature of the ion source and interface was $250\text{ }^{\circ}\text{C}$ and $280\text{ }^{\circ}\text{C}$, respectively. The solvent delay was set to 3.5 min. Identification of the phytochemicals of EOs was based on the comparison of their mass spectra with those of National Institute Standard and Technology version-05 and 05s (NIST 05 and NIST 05s) library data.

2.3. Encapsulation procedure

The co-precipitation method using β -CD was applied according to the methodology described by Ayala-Zavala *et al.*⁵¹ with a few modifications. A total of 2.5 g (± 0.01 g) of β -CD (Wako 1st Grade, FUJIFILM Wako Chemicals, Japan) were dissolved in 50 mL of a co-solvent of ethanol and distilled water (1 : 2 v/v) mixture at $55\text{ }^{\circ}\text{C}$ ($\pm 2\text{ }^{\circ}\text{C}$) and 700 rpm on a hot stirrer plate. In addition, another co-solvent was prepared with 0.1 g (± 0.01 g) oil-in-water emulsifier gum Arabic (referred-to as “GA” hereafter) (AMC. CO., Japan) added with the aim of increasing the dispersibility of EOs in the co-solvent. After cooling the co-solvent to $45\text{ }^{\circ}\text{C}$, 2 mL of the eeHCP(SEEP) was added dropwise using a syringe. Subsequently, the mixture was stirred at $45\text{ }^{\circ}\text{C}$ ($\pm 2\text{ }^{\circ}\text{C}$) for 2 h and then maintained overnight at $4\text{ }^{\circ}\text{C}$ (± 2



°C). The cold precipitates (supposed to be β -CD-eeHCP(SEEP) and β -CD-GA-eeHCP(SEEP) capsules) were recovered *via* the suction filtration and rinsed with 60% ethanol to remove the residual eeHCP(SEEP), and then the capsules were dried in a desiccator at 23 °C for 72 h and stored in an airtight glass at 23 °C before subsequent characterization. As a control, blank β -CD capsules without the addition of eeHCP(SEEP) were prepared in the same condition and steps as mentioned above.

2.4. Physicochemical characterization of capsules

2.4.1. Morphological and dimensional analyses. The morphological structures and particle size of the β -CD-eeHCP(SEEP) and β -CD-GA-eeHCP(SEEP) capsules fabricated by the co-precipitation method were observed using a scanning electron microscopy (SEM) (TM4000Plus, Hitachi, Japan) in the backscattered electron (BSE) mode at a low-vacuum condition to diminish volatilization of phytochemicals inside the capsules. The capsules were coated with platinum for high conductivity prior to the observation and imaged at 10 kV.

2.4.2. X-ray diffraction analysis (XRD). The variation in crystal structure or orientation of capsules before and after encapsulation was confirmed using an X-ray diffractometer (D8 ADVANCE/TSM, Bruker AXS, USA). The XRD patterns were obtained using Cu-K α radiation, at an accelerated voltage of 40 kV and a current of 40 mA. All scans were performed at the 2θ angle ranging between 2 and 30° with an increment of 0.02°.

2.4.3. Fourier transform-infrared analysis (FT-IR). Molecular interactions of capsules between the eeHCP(SEEP) and β -CD were confirmed *via* a Fourier transform-infrared spectroscopy (FT/IR-6800, JASCO, Japan). The FT-IR spectra were collected between 4000 and 400 cm⁻¹ at a resolution of 4 cm⁻¹ with averaging from 16 scans. Liquid eeHCP(SEEP) was pasted on a potassium bromide (KBr) plate; solid β -CD and capsules were ground with KBr powders (approx. 50 mg dry KBr added per 1 mg of solid samples) and then pressed into a 1 mm thick pellet. Raw data of FT-IR spectra were smoothed, and the baseline was corrected *via* the built-in software of the spectrophotometer.

2.5. Antibacterial assay

2.5.1. Antibacterial assessment of extracts. Disk diffusion tests were carried out for the antibacterial evaluation of various extracts obtained by the MCE method and SEEP method. A certain amount of *B. subtilis* (ATCC 19659, Microbiologics, Inc., USA), as the testing microorganism, was picked up using a wire loop and diluted with sterile water. A total of 15 mL sterilized tryptic soy agar (TSA) (Geno Technology Inc. USA) was poured into a Petri dish (Greiner Bio-One International GmbH, Austria) with a diameter of 96 mm. A total of 100 μ L of diluted *B. subtilis* was inoculated into the Petri dish and dispersed evenly using a wire loop. Paper disks with a diameter of 8 mm (Lot No. 50909691, Advantec, Toyo Roshi Kaisha, Ltd., Japan) were impregnated with all extracts obtained by two extraction methods, separately for 5 min. After that, all paper disks were taken out and air-dried for 5 min to eliminate a potential impact from solvents (such as ethanol). To inspect whether the step of

air-drying for 5 min was sufficient to eliminate the impact from solvents on the growth of *B. subtilis*, a blank paper disk impregnated with 99.5% ethanol and then air-dried for 5 min was set as a control. Finally, all paper disks were placed on the *B. subtilis*-inoculated Petri dish, which was then sealed with a Riken wrap and incubated at 37 °C for 24 h. All operations were carried out in a clean bench (CCV-811, Hitachi, Japan).

2.5.2. Antibacterial assessment of capsules. A total of 15 mL sterilized TSA with 0.075 g (\pm 0.001 g) of fabricated capsules was poured simultaneously into a Petri dish to achieve a capsule content of 5 g L⁻¹. A total of 10 μ L of diluted *B. subtilis* at two different concentrations ascertained by a flat colony counting method was inoculated in the centre of the Petri dish. After that, the Petri dish was sealed with a Riken wrap and incubated at 37 °C for a certain period to evaluate the antibacterial activity from the aspect of the growth and breeding of *B. subtilis*. All operations were carried out in the clean bench. The plain β -CD and the blank capsules without the addition of eeHCP(SEEP) were set as controls.

2.6. Statistical analysis

This study was carried out based on a completely randomized design with equal replication. All values were conducted in triplicate and reported as the mean \pm standard deviation. For antibacterial evaluation of various extracts obtained by the MCE method and SEEP method, the area of inhibitory zone was measured with ImageJ 1.53e software in consideration of the asymmetrical appearance. The results were analysed for statistical significance *via* one-way analysis of variance (ANOVA) with Statistical Package of the Social Science (SPSS) version 28.0 (IBM Corporation, USA) software. Significant differences at a level of $p < 0.05$ were identified by the least significant difference (LSD) test.

3 Results and discussion

3.1. Antibacterial activity of various extracts

Table 2 shows the antibacterial activity statistical analysis of various extracts through the growth inhibition against *B. subtilis*. No inhibitory zone was observed with the blank paper disk which was impregnated with 99.5% ethanol and then air-dried for 5 min, indicating that the step of air-drying for 5 min was sufficient to eliminate the impact from solvents on the growth of *B. subtilis*. Among the extracts obtained by the MCE method,

Table 2 Area of inhibitory zone of various HC extracts against *B. subtilis*

Sample	Area of inhibition zone (mm ²)
Blank paper disk	0
heHC(MCE)	130 \pm 15
eeeHC(MCE)	750 \pm 29
eeHC(MCE)	316 \pm 14
eeHCP(SEEP)	712 \pm 24
eeHC(SEEP)	234 \pm 25



it is obvious that the best inhibition against *B. subtilis* was achieved by the eeeHC(MCE), followed by the eeHC(MCE), and then the heHC(MCE). It is assumed that greases and some proteins can be removed primarily with hexane; some active phytocompounds of EOs containing a certain amount of hydroxyl or carboxyl groups resemble ethyl ether in polarity can be removed with ethyl ether and lastly the remaining constituents such as alkaloids and organic acids are supposed to be separated out in ethanol. The experimental results demonstrated the above notion that the eeeHC(MCE) containing a large amount of EOs exhibited the superb inhibitory effect on the growth of *B. subtilis*. However, the polarity of some active phytocompounds of EOs such as 2-undecanone and β -myrcene are positioned between ethyl ether and hexane and might be partially extracted in hexane, accounting for why heHC(MCE) showed a certain inhibitory effect as well. A prominent inhibitory effect was also noted in eeHC(MCE), probably due to the amount of ethyl ether used was too small to extract all EOs, resulting in a partial flow of active phytocompounds into the eeHC(MCE), and consequently an inhibitory effect appeared in the eeHC(MCE). Therefore, if the extraction time of hexane was reduced and the amount of ethyl ether was increased, the antibacterial activity of eeeHC(MCE) might have greater enhancement, then further experiment is required to confirm whether it is true or false.

As to the SEEP method, the inhibitory effect of eeHCP(SEEP) was much superior to that of eeHC(SEEP) which was set as a control, presumably because the process of heating for a short time was considered to be a simple operation like steam distillation, which might reduce the EOs leaching resistance during the vortex.⁵⁰ This clarifies why the inhibitory effect of eeHCP(SEEP) (approx. 710 mm² of inhibition zone) was close to that of eeeHC(MCE) (approx. 750 mm² of inhibition zone). Nevertheless, from the perspective of operational, economic and environmental aspects, eeHCP(SEEP) seems to be more advantageous, and therefore only eeHCP(SEEP) was chosen for the subsequent encapsulation procedure.

Although eeHCP(SEEP) exhibited satisfactory results, the use of ethanol as solvent led to a large number of constituents extracted from HC. Thus, vortex (extraction) time ought to be an exceptionally critical factor. To further investigate the impact of vortex time, an antibacterial assay was performed using a certain amount of *B. subtilis*. Fig. 1 shows the antibacterial activity of eeHCP(SEEP) with an increased vortex time and eeHC(SEEP) was set as a comparison. By vortex at high frequencies, EOs were extracted rapidly due to the pre-treatment of heating and their property of high volatility. Therefore, the vortex time should be adjusted to warrant a maximum possible, while not excessive or insufficient EOs extraction, otherwise other compounds would emerge or inadequate EOs contents might reduce the concentration of EOs in the extract, thus reducing the overall antibacterial activity. Evidently, for both eeHCP(SEEP) and eeHC(SEEP), a maximum area of the inhibitory zone was attained at a vortex time of 3 min, and hence the eeHCP(SEEP) obtained at this vortex time was chosen for the subsequent encapsulation procedure. In addition, Fig. 2 shows a comparison in the area of inhibitory

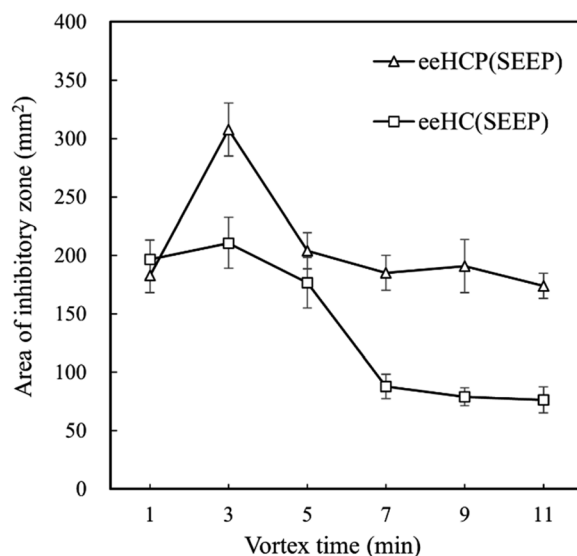


Fig. 1 Area of inhibitory zone of eeHCP(SEEP) and eeHC(SEEP) versus vortex time after incubation at 37 °C for 24 h.

zone of eeHCP(SEEP) after incubation for 24 h and 72 h. The area was slightly smaller after incubation for 72 h than that for 24 h, ensuring a strong antibacterial activity of eeHCP(SEEP) against *B. subtilis*.

3.2. GC-MS analysis

eeHCP(SEEP) and eeHC(SEEP) which was set as a control were subjected to GC-MS analysis. A total of 168 phytocompounds from eeHCP(SEEP) and 185 phytocompounds from eeHC(SEEP) were identified by GC-MS, separately. Fig. 3 shows total ion chromatograms (TIC) of eeHCP(SEEP) and eeHC(SEEP). The integrated peak area of top 50 phytocompounds which occupied more than 98% of the overall area in each of TIC, are selected

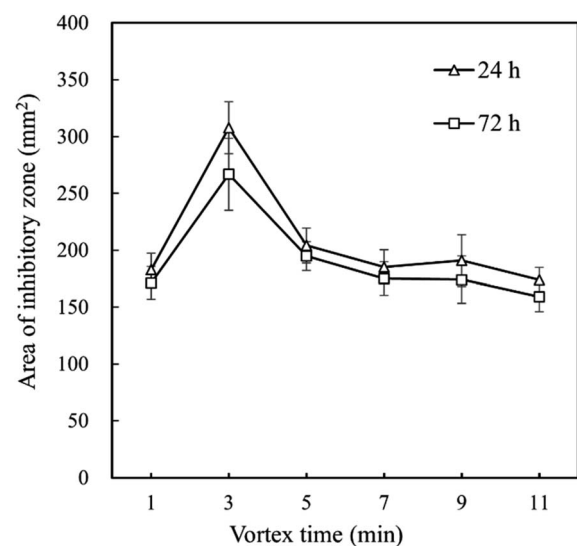


Fig. 2 Difference in the area of inhibitory zone of eeHCP(SEEP) versus vortex time after incubation at 37 °C for 24 h and 72 h.



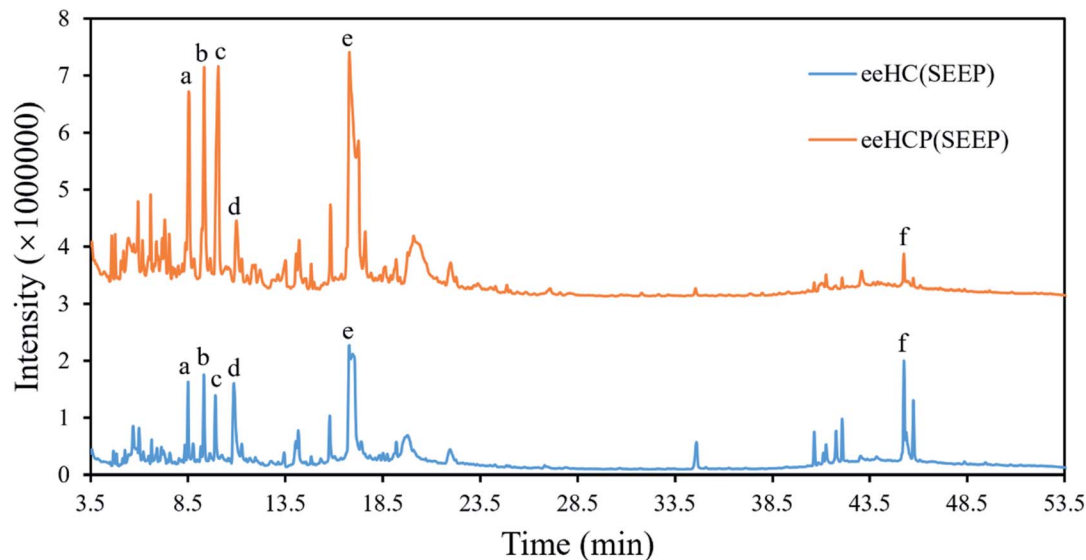


Fig. 3 Total ion chromatogram of eeHCP(SEEP) and eeHC(SEEP).

for display in Table 3. Altogether, 26 identical phytochemicals were identified. Visually, the TIC of eeHCP(SEEP) was similar to that of eeHC(SEEP), but there was a slight difference. The intensity of phytochemicals detected from eeHCP(SEEP) was distinctly higher than that of eeHC(SEEP) during the retention time from 4 to 20 min, while the opposite result was noticed from 39 to 46 min. Six typical phytochemicals *a*, *b*, *c*, *d*, *e* and *f* labelled in Fig. 3 correspond to 4H-Pyran-4-one, 2,3-dihydro-3,5-dihydroxy-6-methyl- (No 5), decanal (No 3), 2-furancarboxaldehyde, 5-(hydroxymethyl)- (No 2), hydroquinone (No 7), 4-tridecanone (No 1) and 9-octadecanamide, (*Z*)- (No 22) are shown in Table 3. Of these, peak area of phytochemicals *a* (5.63%), *b* (7.48%), *c* (8.96%) and *e* (19.00%) were higher in eeHCP(SEEP) than *a* (3.42%), *b* (3.53%), *c* (3.89%) and *e* (8.91%) in eeHC(SEEP) respectively, whereas *d* (2.71%) and *f* (0.55%) were lower in eeHCP(SEEP) than *d* (7.41%) and *f* (6.39%) in eeHC(SEEP). According to the reports of Yang *et al.*³³ and Wu *et al.*,³⁴ decanal and its derivatives play an extremely crucial role in acting antibacterial activity, which therefore clarifies why the antibacterial activity of eeHCP(SEEP) was much greater than that of eeHC(SEEP). One additional finding was that some phytochemicals detected in eeHCP(SEEP) but not in eeHC(SEEP) had structural similarities to the phytochemicals detected in eeHC(SEEP) but not in eeHCP(SEEP), such as No 32 and No 65, with the main difference being the variation of the individual functional groups, which could be elucidated by that some of the substances underwent structural changes as a result of the pre-heating in the eeHCP(SEEP) preparation.

3.3. Morphological and dimensional analyses of capsules

The β -CD-eeHCP(SEEP) and β -CD-GA-eeHCP(SEEP) capsules obtained by the co-precipitation method were in powder form after drying and the SEM images of them are shown in Fig. 4. Plain β -CD (Fig. 4a) as purchased was characterized as homogeneous massive or lamellar plates with well-grown crystals in varying sizes. However, the shape of the blank β -CD capsules

(Fig. 4b) without the addition of eeHCP(SEEP) was not consistent with that of plain β -CD and appeared to be more granular in shape. Actually, the blank β -CD capsules were obtained through a process in which plain β -CD was dissolved in the co-solvent and then precipitated, suggesting a condition like precipitation rate caused some alteration in the particle shape of recovered β -CD, in consistency with the findings of Nakai *et al.*⁵² who also confirmed that water molecules exert an influence on the crystal structure of cyclodextrins. This is why the surface of the β -CD-eeHCP(SEEP) capsules (Fig. 4c) and β -CD-GA-eeHCP(SEEP) (Fig. 4d) resembled that of blank β -CD capsules rather than the plain β -CD. It is observed that β -CD-eeHCP(SEEP) capsules and β -CD-GA-eeHCP(SEEP) capsules had extremely similar cubic and irregular structures with the dimensions of approx. 80 μ m in diameter and exhibited clustering, as was likewise reported by Saucieu *et al.*⁵³ The original intention of the addition of GA as an emulsifier to the co-solvent was to improve the dispersion of the EOs in the co-solvent, but in terms of experimental results, the same objective was achieved without the addition of GA. This was attributed to the ethanol in the co-solvent. Not only did the ethanol improve the solubility of β -CD (only about 1.5 g β -CD can be dissolved in 50 mL of water-solvent in the same condition described in Section 2.3) and thus increased the efficiency of encapsulation, but also it contributed to the dispersion of the EOs in the co-solvent. However, it is also important that a high content of ethanol may assist the dissolution of some EOs phytochemicals in the co-solvent rather than being embedded within hollow cavities of β -CD, so an optimum ratio of water to ethanol needs further experimentation.

3.4. XRD analysis

XRD is a useful method for the detection of crystalline states. Fig. 5 shows the XRD patterns of capsules produced by the co-precipitation method. The XRD pattern of blank β -CD capsules (Fig. 5b) was almost identical to those of β -CD-



Table 3 List of top 50 phytocompounds identified from eeHCP(SEEP) and eeHC(SEEP) via GC-MS^{ab}

No	Phytocompound name	Peak area (%)	
		eeHCP(SEEP)	eeHC(SEEP)
1	4-Tridecanone	19.00 ± 0.85	8.91 ± 0.48
2	2-Furancarboxaldehyde, 5-(hydroxymethyl)-	8.96 ± 0.52	3.89 ± 0.41
3	Decanal	7.48 ± 0.47	3.53 ± 0.40
4	Benzoic acid, 3-hydroxy-	6.36 ± 0.46	14.69 ± 1.88
5	4H-Pyran-4-one, 2,3-dihydro-3,5-dihydroxy-6-methyl-	5.63 ± 1.05	3.42 ± 0.14
6	Megastigmatrienone	3.59 ± 0.02	0.58 ± 0.04
7	Hydroquinone	2.71 ± 0.12	7.41 ± 0.37
8	2,4-Dihydroxy-2,5-dimethyl-3(2H)-furan-3-one	2.22 ± 0.08	1.56 ± 0.07
9	Benzaldehyde, 2-hydroxy-4-methyl-	1.81 ± 0.06	2.80 ± 0.43
10	2H-Pyran-2,6(3H)-dione	1.40 ± 0.46	0.78 ± 0.05
11	Benzoic acid, 4-hydroxy-	1.67 ± 0.10	1.26 ± 0.03
12	<i>n</i> -Decanoic acid	1.59 ± 0.16	0.88 ± 0.05
13	14-Bromo-2-methyltetradec-1-en-3-ol	1.41 ± 0.07	2.10 ± 0.00
14	2,5-Dimethyl-4-hydroxy-3(2H)-furanone	1.36 ± 0.08	0.85 ± 0.04
15	β-Myrcene	1.07 ± 0.07	2.81 ± 0.73
16	Methyl 2-furoate	1.05 ± 0.04	0.58 ± 0.02
17	Decanoic acid, ethyl ester	0.93 ± 0.04	1.13 ± 0.07
18	Ethanamine, 2-methoxy- <i>N</i> -(2-methoxyethyl)- <i>N</i> -methyl-	0.87 ± 0.05	0.70 ± 0.02
19	Benzenecarboxylic acid	0.70 ± 0.12	1.20 ± 0.05
20	Oxime-, methoxy-phenyl-	0.74 ± 0.06	0.39 ± 0.04
21	3-Hydroxy-4-methoxybenzoic acid	0.64 ± 0.14	0.33 ± 0.02
22	9-Octadecenamide, (Z)-	0.55 ± 0.09	6.39 ± 0.33
23	2-Undecanone	0.56 ± 0.03	1.51 ± 0.51
24	Dodecanal	0.51 ± 0.03	0.34 ± 0.02
25	1,2-Cyclopentanedione	0.52 ± 0.01	0.43 ± 0.09
26	Octadecanamide	0.34 ± 0.02	2.99 ± 0.30
27	1,2,3,5-Cyclohexanetetrol, (1α, 2β, 3α, 5β)-	4.69 ± 0.40	0
28	2-Furancarboxaldehyde, 5-methyl-	3.29 ± 1.01	0
29	4-Ethylcatechol	1.77 ± 0.10	0
30	3-Furancarboxylic acid	1.67 ± 0.01	0
31	Thiophene, 2-formyl-2,3-dihydro-	1.58 ± 0.03	0
32	2,5-Furandione, dihydro-3-methylene-	1.49 ± 0.06	0
33	3-Hydroxy-β-damascone	1.41 ± 0.11	0
34	Ethanone, 1-(2-hydroxy-5-methylphenyl)-	1.21 ± 0.04	0
35	Ethanamine, <i>N</i> -ethyl- <i>N</i> -nitroso-	1.13 ± 0.05	0
36	Bicyclo[3.1.1]heptan-3-ol, 2,6,6-trimethyl-, (1α,2β,3α,5β)-	1.00 ± 0.07	0
37	Ribitol	0.93 ± 0.04	0
38	2,13-Dibora-1,3,6,9,12,14,17,20-octaaxacyclodocosane, 2,13-diethyl-	0.74 ± 0.03	0
39	Benzamide	0.60 ± 0.04	0
40	2(5H)-Furanone	0.62 ± 0.01	0
41	Benzofuran, 2,3-dihydro-	0.55 ± 0.07	0
42	Furan, 2-[(methylthio)methyl]-	0.55 ± 0.03	0
43	Benzyl β- <i>D</i> -glucoside	0.53 ± 0.03	0
44	Octyl-β- <i>D</i> -glucopyranoside	0.46 ± 0.02	0
45	1H-Indene, 2,3-dihydro-1,1,5,6-tetramethyl-	0.42 ± 0.02	0
46	Naphthalene, 1,2-dihydro-2,5,8-trimethyl-	0.41 ± 0.01	0
47	Pyrimidine-4,6-diol, 5-methyl-	0.36 ± 0.02	0
48	Nonane, 1,1-diethoxy-	0.36 ± 0.01	0
49	9,12,15-Octadecatrienoic acid, methyl ester, (Z,Z,Z)-	0.28 ± 0.07	0
50	1,3-Cyclohexanedione, 2-methyl-	0.28 ± 0.05	0
51	(1R,3R,4R,5R)-(-)-Quinic acid	0	5.74 ± 0.10
52	Pentadecanoic acid	0	1.84 ± 0.16
53	1,3-Benzenediol, 4-ethyl-	0	1.70 ± 0.26
54	Hexadecanamide	0	1.62 ± 0.16
55	1,2,3-Benzenetriol	0	1.73 ± 0.03
56	Octadecanoic acid	0	1.55 ± 0.19
57	Phytol	0	1.34 ± 0.06
58	Cyclopentene, 1,2-dimethyl-4-methylene-	0	1.19 ± 0.03
59	Thiophene, 2-methoxy-5-methyl-	0	1.09 ± 0.11
60	Phenol	0	1.07 ± 0.10
61	Dichloroacetic acid, tridec-2-ynyl ester	0	0.98 ± 0.06



Table 3 (Contd.)

No	Phytocompound name	Peak area (%)	
		eeHCP(SEEP)	eeHC(SEEP)
62	2-Furancarboxylic acid	0	0.97 ± 0.05
63	2-Benzyl-2-methyl-1,3-oxathiolane	0	0.84 ± 0.10
64	Ethanamine, <i>N</i> -ethyl- <i>N</i> -nitroso-	0	0.90 ± 0.03
65	2,5-Furandione, 3-methyl-	0	0.85 ± 0.02
66	4H-Pyran-4-one, 3,5-dihydroxy-2-methyl-	0	0.78 ± 0.07
67	1,4:3,6-Dianhydro- α - <i>D</i> -glucopyranose	0	0.83 ± 0.02
68	4-Benzoyloxy-1-morpholinocyclohexene	0	0.71 ± 0.03
69	9,12-Octadecadienoic acid, methyl ester	0	0.68 ± 0.02
70	1,3,6-Octatriene, 3,7-dimethyl-, (E)-	0	0.55 ± 0.03
71	3-Chloropropionic acid, 2,6-dimethylnon-1-en-3-yn-5-yl ester	0	0.53 ± 0.01
72	Isolongifolan-8-ol	0	0.38 ± 0.05
73	Bendiocarb	0	0.32 ± 0.07
74	3-Ethyl-3-heptanol	0	0.33 ± 0.04
Total (%)		100	100

^a Note: 1 A Peak area of 0% does not mean non-existence but not included in the top 50 phytocompounds of eeHCP(SEEP) or eeHC(SEEP). ^b 2 The peak area ratio of each phytocompound was calculated based on the sum of the peak area of the top 50 phytocompounds assumed to be 100%.

eeHCP(SEEP) capsules (Fig. 5c) and β -CD-GA-eeHCP(SEEP) (Fig. 5d), while it was similar to that of plain β -CD (Fig. 5a) in the peak position (2θ) but with different peak intensity mutually. The diffraction angle 2θ of the plain β -CD had intense and sharp peaks at 11.32, 14.47 17.42 and 18.53°. However, in the patterns of blank β -CD capsules, β -CD-eeHCP(SEEP) capsules and β -CD-GA-eeHCP(SEEP) capsules, these peaks were substantially compressed, despite heightened peaks at 10.43, 12.24 and 19.45°. This is because crystallites of the β -CD become oriented upon precipitation, just as discussed in the

SEM section, and the presence or absence of eeHCP(SEEP) did not alter the crystal orientation of the capsules, in line with the results reported by Munhuweyi *et al.*⁵⁴ who observed the same XRD patterns of capsules produced *via* employing two different kinds of EOs.

3.5. FT-IR analysis

FT-IR was used to demonstrate the interaction between β -CD and eeHCP(SEEP) in the process of forming capsules in terms of peak shape, position and intensity. Fig. 6 shows the FT-IR

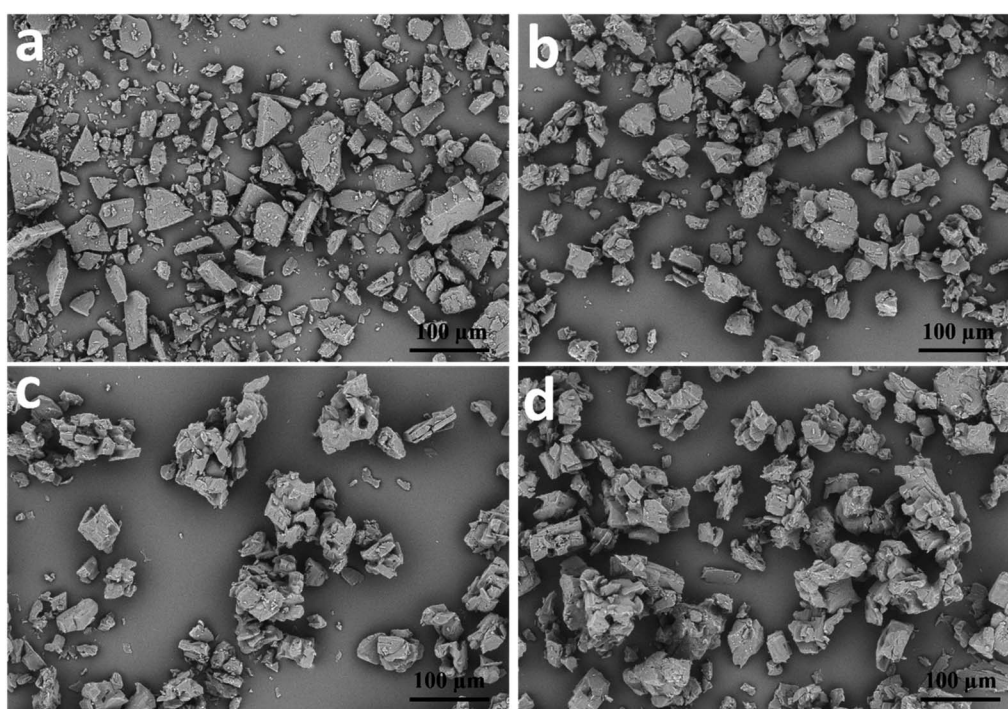


Fig. 4 SEM images of plain β -CD (a), blank β -CD capsules (b), β -CD-eeHCP(SEEP) capsules (c) and β -CD-GA-eeHCP(SEEP) capsules (d).



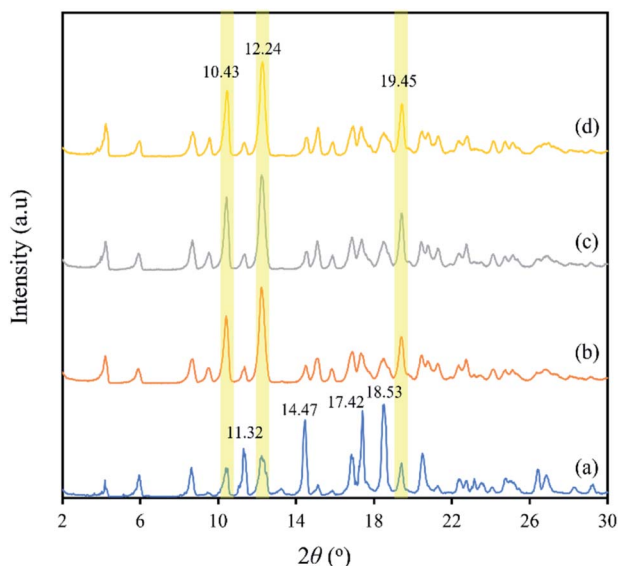


Fig. 5 XRD patterns of plain β -CD (a), blank β -CD capsules (b), β -CD-eeHCP(SEEP) capsules (c) and β -CD-GA-eeHCP(SEEP) capsules (d).

spectra of eeHCP(SEEP) (Fig. 6a), plain β -CD (Fig. 6b), blank β -CD capsules (Fig. 6c), β -CD-eeHCP(SEEP) capsules (Fig. 6d) and β -CD-GA-eeHCP(SEEP) capsules (Fig. 6e). Typically, eeHCP(SEEP) exhibited three characteristic peaks at 3355.5 cm^{-1} (for O–H stretching vibrations), 2922.6 cm^{-1} (for C–H stretching vibrations), and a prominent absorption peak at 1630.5 cm^{-1} (for C=O stretching vibration of amides). The absorption bands of plain β -CD were observed at 3369.0 , 2924.5 , 1649.9 , 1157.1 and 1028.8 cm^{-1} , corresponding to the vibration of symmetrical and asymmetrical stretching of the O–H, C–H stretching vibrations, H–O–H bending, C–O stretching vibration, and

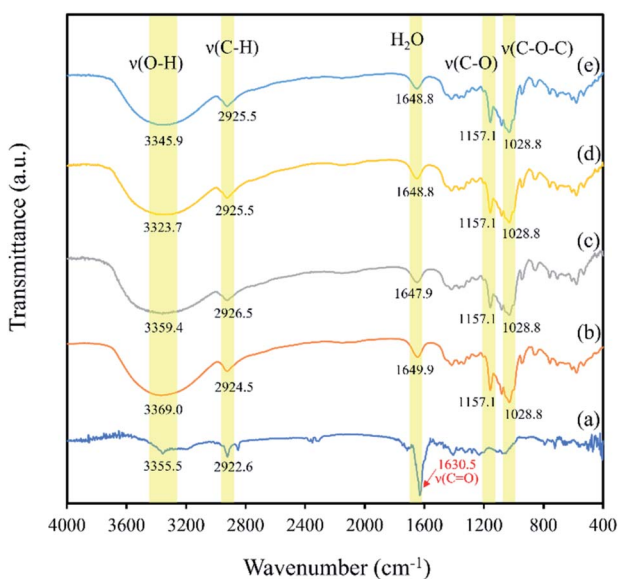


Fig. 6 FT-IR spectra of eeHCP(SEEP) (a), plain β -CD (b), blank β -CD capsules (c), β -CD-eeHCP(SEEP) capsules (d) and β -CD-GA-eeHCP(SEEP) capsules (e).

symmetric stretching link C–O–C, respectively.⁵⁵ Obviously, the FT-IR spectra of blank β -CD capsules, β -CD-eeHCP(SEEP) capsules as well as β -CD-GA-eeHCP(SEEP) capsules revealed a high degree of similarity to the spectra of plain β -CD, except for the position of O–H absorption peaks which shifted towards lower frequencies. Kayaci *et al.*⁵⁶ and Del Toro-Sánchez *et al.*⁵⁷ explained these shifts after encapsulation indicated an interaction had occurred between the embedded materials and β -CD *via* hydrogen bonding, however, a slight shift in the position of O–H absorption peak of blank β -CD capsules was also observed, possibly suggesting that the remaining water molecules after drying were likewise hydrogen-bonded to the β -CD. In addition, it is worth noting that the highly intense peak of eeHCP(SEEP) located at 1630.5 cm^{-1} was not detected in the spectra of β -CD-eeHCP(SEEP) and β -CD-GA-eeHCP(SEEP) capsules in consistent with the findings reported by Wang *et al.*⁵⁵ and Munhuweyi *et al.*⁵⁴ who considered this was due to the successful encapsulation by β -CD, however, it should be evidenced in conjunction with a subsequent antibacterial assay. Moreover, combined with the results of SEM, XRD and FT-IR, with the addition of GA as an emulsifier to the co-solvent, no significant change was observed, possibly because the presence of ethanol in the co-solvent was sufficient to achieve a good dispersibility of EOs, just as discussed in the Section 3.3. Therefore, it could be considered that GA was not required to the co-solvent in this study and only the β -CD-eeHCP(SEEP) capsules were used for the antibacterial assay.

3.6. Antibacterial activity of capsules

To investigate the antibacterial activity of the fabricated capsules, an antibacterial assay using *B. subtilis* as a study object was performed. The growth and breeding status of *B. subtilis* in TSA medium with the addition of plain β -CD (a), blank β -CD capsules (b) and β -CD-eeHCP(SEEP) capsules (c) was observed after an addition of $10\text{ }\mu\text{L}$ diluted *B. subtilis* at two different concentrations, as shown in Fig. 7 ($6 \times 10^4\text{ CFU mL}^{-1}$) and Fig. 8 ($6 \times 10^6\text{ CFU mL}^{-1}$), respectively. Plain β -CD and blank β -CD capsules resulted in a rapid growth and breeding of *B. subtilis* due to the fact that β -CD is a polysaccharide that can provide a carbohydrate source and blank β -CD capsules were merely the precipitated product of dissolved β -CD. On the contrary, the addition of capsules containing eeHCP(SEEP) showed a potent inhibitory ability. There appeared to be a slight difference after incubation for 24 h in the growth of *B. subtilis* among the addition of plain β -CD, blank β -CD capsules and β -CD-eeHCP(SEEP) capsules; however, when the incubation was continued to 48 h, a distinctive difference was reflected. Also, remarkably similar results were exhibited whether the concentration of *B. subtilis* added was 6×10^4 or $6 \times 10^6\text{ CFU mL}^{-1}$. This fact indirectly revealed the eeHCP(SEEP) was successfully encapsulated within hollow cavities of β -CD, as estimated from the FT-IR spectra. Most importantly, this satisfactory antibacterial activity of the β -CD-eeHCP(SEEP) capsules fabricated by the co-precipitation method in this study provides a promising direction for the use of eco-friendly antibacterial agents for food packaging industry.



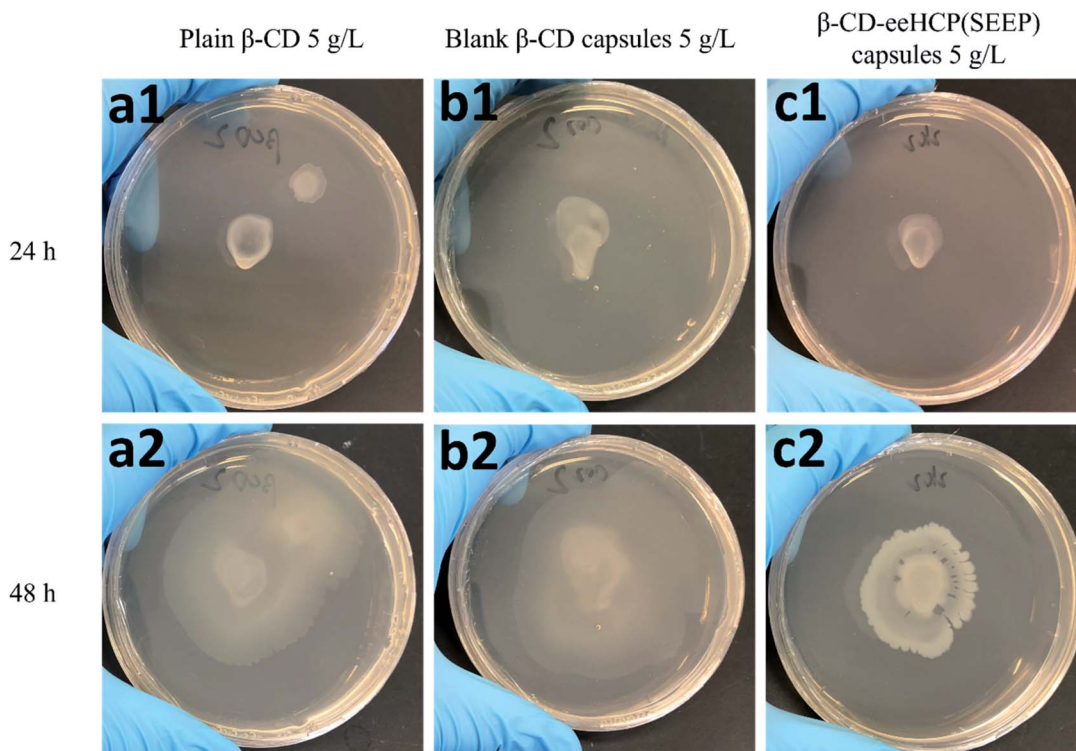


Fig. 7 Growth of $10 \mu\text{L } 6 \times 10^4 \text{ CFU mL}^{-1}$ *B. subtilis* with plain β -CD (a), blank β -CD capsules (b) and β -CD-eeHCP(SEEP) capsules (c) after incubation for 24 h and 48 h.

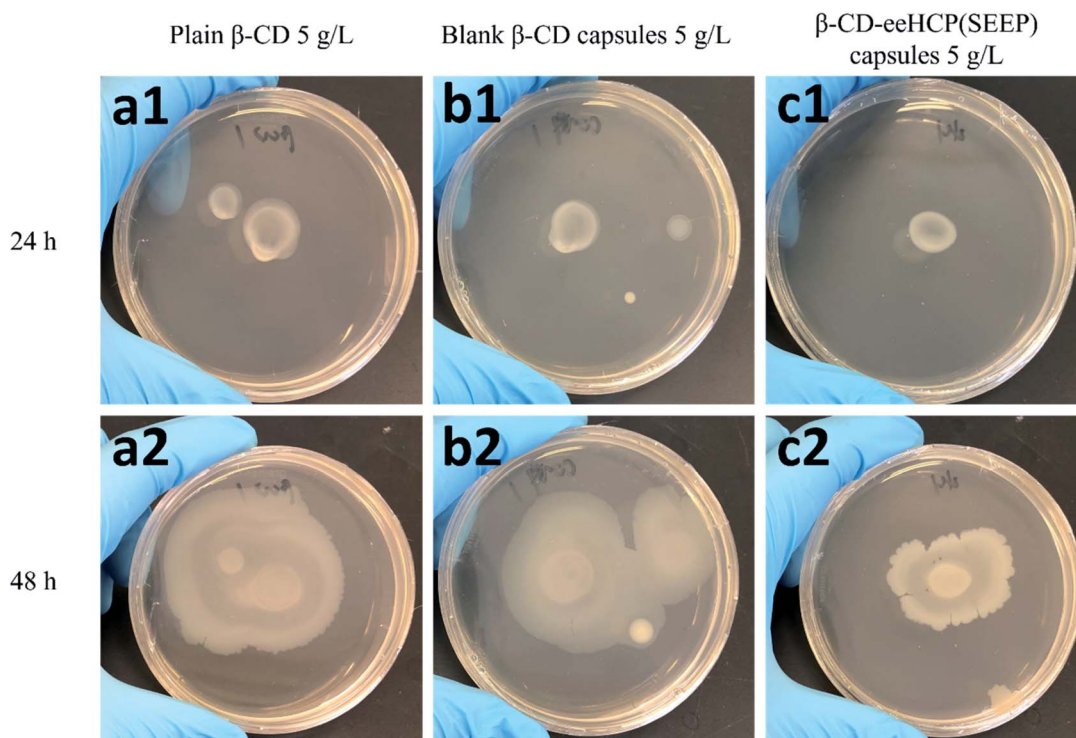


Fig. 8 Growth of $10 \mu\text{L } 6 \times 10^6 \text{ CFU mL}^{-1}$ *B. subtilis* with plain β -CD (a), blank β -CD capsules (b) and β -CD-eeHCP(SEEP) capsules (c) after incubation for 24 h and 48 h.



4 Conclusions

This study developed a promising antibacterial agent containing an HC extract for food packaging. Two extraction methods: MCE method and SEEP method, were attempted to extract EOs from the HC. Although the eeHC(MCE) exhibited the greatest anti-*B. subtilis* activity, the eeHCP(SEEP) was chosen for the capsule synthesis, taking into account the operational and economical aspects.

The results of GC-MS showed the content of decanal which plays a definitely crucial role in the antibacterial activity in eeHCP(SEEP) was higher than that in eeHC(SEEP), explaining a higher antibacterial activity of eeHCP(SEEP). Afterwards, the co-precipitation method using β -CD was employed to produce capsules to protect the EOs of eeHCP(SEEP). Consequently, the fabricated capsules were in powder form with the dimensions of approx. 80 μ m in diameter. The SEM and XRD results showed the β -CD crystallites in form of thinner plates became oriented upon precipitation. From the comprehensive results of SEM, XRD and FT-IR, GA added with the aim of increasing the dispersibility of EOs in the co-solvent was not required in this study due to the presence of ethanol in the co-solvent was sufficient to achieve a good dispersibility of EOs. Combining the results of FT-IR analysis and an antibacterial assay, it is revealed that the eeHCP(SEEP) was successfully encapsulated within hollow cavities of β -CD. Moreover, the antibacterial assay demonstrated a satisfactory antibacterial activity of the fabricated β -CD-eeHCP(SEEP) capsules, making them prospective for food packaging as an eco-friendly antibacterial agent.

Author contributions

P. K. performed most of the experimental work and wrote the manuscript. J. P. A., A. N. and M. K. guided and assisted in part of the experiments. T. E. supervised the whole study and revised the manuscript. All authors have given final approval to publish the manuscript.

Conflicts of interest

There are no conflicts to declare.

Acknowledgements

We would like to thank the Open Facility Centre, University of Tsukuba for allowing us to use their facilities. The authors are also thankful to the Academic Computing & Communications Centre, University of Tsukuba for providing the SPSS software.

References

- 1 Y. Ma, P. Liu, C. Si and Z. Liu, *J. Macromol. Sci., Part B: Phys.*, 2010, **49**, 994–1001.
- 2 T.-T. Tsai, T.-H. Huang, C.-J. Chang, N. Yi-Ju Ho, Y.-T. Tseng and C.-F. Chen, *Sci. Rep.*, 2017, **7**, 1–10.
- 3 P. J. P. Espitia, N. d. F. F. Soares, R. F. Teófilo, J. S. dos Reis Coimbra, D. M. Vitor, R. A. Batista, S. O. Ferreira, N. J. de Andrade and E. A. A. Medeiros, *Carbohydr. Polym.*, 2013, **94**, 199–208.
- 4 M. Carbone, D. T. Donia, G. Sabbatella and R. Antiochia, *J. King Saud Univ., Sci.*, 2016, **28**, 273–279.
- 5 N. C. Martins, C. S. Freire, C. P. Neto, A. J. Silvestre, J. Causio, G. Baldi, P. Sadocco and T. Trindade, *Colloids Surf., A*, 2013, **417**, 111–119.
- 6 N. Omerović, M. Djisalov, K. Živojević, M. Mladenović, J. Vunduk, I. Milenković, N. Ž. Knežević, I. Gadjanski and J. Vidić, *Compr. Rev. Food Sci. Food Saf.*, 2021, **20**, 2428–2454.
- 7 Z. Wu, X. Huang, Y. C. Li, H. Xiao and X. Wang, *Carbohydr. Polym.*, 2018, **199**, 210–218.
- 8 T.-T. Tsai, T.-H. Huang, C.-J. Chang, N. Yi-Ju Ho, Y.-T. Tseng and C.-F. Chen, *Sci. Rep.*, 2017, **7**, 3155.
- 9 P. Kanmani and J.-W. Rhim, *Food Chem.*, 2014, **148**, 162–169.
- 10 A. Ben Arfa, L. Preziosi-Belloy, P. Chalier and N. Gontard, *J. Agric. Food Chem.*, 2007, **55**, 2155–2162.
- 11 L. Motelica, D. Ficaí, A. Ficaí, R.-D. Truşcă, C.-I. Ilie, O.-C. Oprea and E. Andronescu, *Foods*, 2020, **9**, 1801.
- 12 L. Motelica, D. Ficaí, O.-C. Oprea, A. Ficaí, V.-L. Ene, B.-S. Vasile, E. Andronescu and A.-M. Holban, *Nanomaterials*, 2021, **11**, 2377.
- 13 L. Motelica, D. Ficaí, O. Oprea, A. Ficaí, R.-D. Trusca, E. Andronescu and A. M. Holban, *Pharmaceutics*, 2021, **13**, 1020.
- 14 V. G. L. Souza, C. Rodrigues, S. Valente, C. Pimenta, J. R. A. Pires, M. M. Alves, C. F. Santos, I. M. Coelho and A. L. Fernando, *Coatings*, 2020, **10**, 110.
- 15 R. Ribeiro-Santos, M. Andrade and A. Sanches-Silva, *Curr. Opin. Food Sci.*, 2017, **14**, 78–84.
- 16 P. S. G. R. a. Safe, *U.S. Food and Drug Administration*, 2022, Title 21-Food and Drugs, <https://www.accessdata.fda.gov/scripts/cdrh/cfdocs/cfcfr/CFRSearch.cfm?CFRPart=182>.
- 17 T. Nakatsu, A. T. Lupo Jr, J. W. Chinn Jr and R. K. Kang, in *Studies in natural products chemistry*, Elsevier, 2000, vol. 21, pp. 571–631.
- 18 J. Dai and R. J. Mumper, *Molecules*, 2010, **15**, 7313–7352.
- 19 J. S. Raut and S. M. Karuppayil, *Ind. Crops Prod.*, 2014, **62**, 250–264.
- 20 A. C. Gargano, C. Costa and M. Costa, *Tree For. Sci. Biotechnol.*, 2008, **2**, 121–124.
- 21 E. F. de Matos, B. S. Scopel and A. Dettmer, *J. Environ. Chem. Eng.*, 2018, **6**, 1989–1994.
- 22 Z. Xiao, W. Liu, G. Zhu, R. Zhou and Y. Niu, *J. Sci. Food Agric.*, 2014, **94**, 1482–1494.
- 23 D. Poncet in *Surface chemistry in biomedical and environmental science*, Springer, 2006, pp. 23–34.
- 24 W. Li, G. Wu, H. Chen and M. Wang, *Colloids Surf., A*, 2009, **333**, 133–137.
- 25 J. Oxley in *Microencapsulation in the food industry*, Elsevier, 2014, pp. 35–46.
- 26 S. Freiberg and X. Zhu, *Int. J. Pharm.*, 2004, **282**, 1–18.
- 27 S. Freitas, H. P. Merkle and B. Gander, *J. Controlled Release*, 2005, **102**, 313–332.
- 28 H. Sawalha, K. Schroen and R. Boom, *Chem. Eng. J.*, 2011, **169**, 1–10.



- 29 P. S. Elizei and W. Krasaaekoopt, *Agric. Nat. Resour.*, 2014, **48**, 893–907.
- 30 M. G. Bah, H. M. Bilal and J. Wang, *Soft Matter*, 2020, **16**, 570–590.
- 31 M. Peanparkdee, S. Iwamoto and R. Yamauchi, *Reviews in Agricultural Science*, 2016, **4**, 56–65.
- 32 X. Pan, H. Li, D. Chen, J. Zheng, L. Yin, J. Zou, Y. Zhang, K. Deng, M. Xiao and L. Meng, *Int. J. Anal. Chem.*, 2021, 2021.
- 33 L. Yang and J.-G. Jiang, *Pharm. Biol.*, 2009, **47**, 1154–1161.
- 34 Z. Wu, X. Deng, Q. Hu, X. Xiao, J. Jiang, X. Ma and M. Wu, *Front. Pharmacol.*, 2021, 12.
- 35 J. Pharmacopoeia, *Pharmaceuticals and Medical Devices Agency*, 2021, 18th, <https://www.pmda.go.jp/english/rs-sb-std/standards-development/jp/0029.html>.
- 36 S. K. Das, S. Mahanta, B. Tanti, H. Tag and P. K. Hui, *Mol. Diversity*, 2021, 1–24.
- 37 M. Zeng, L. Li and Z. Wu, *PLoS One*, 2020, **15**, e0238828.
- 38 J. Fu, L. Dai, Z. Lin and H. Lu, *Chin. Med.*, 2013, **4**, 101–123.
- 39 M. Kumar, S. K. Prasad and S. Hemalatha, *Pharmacogn. Rev.*, 2014, **8**, 22–35.
- 40 H. D. Kwon, I. H. Cha, W. K. Lee, J. H. Song and I. H. Park, *Prev. Nutr. Food Sci.*, 1996, **1**, 208–213.
- 41 A. Arana-Sánchez, M. Estarrón-Espinosa, E. Obledo-Vázquez, E. Padilla-Camberos, R. Silva-Vázquez and E. Lugo-Cervantes, *Lett. Appl. Microbiol.*, 2010, **50**, 585–590.
- 42 M. Kfoury, L. Auezova, H. Greige-Gerges and S. Fourmentin, *Carbohydr. Polym.*, 2015, **131**, 264–272.
- 43 M. Karaaslan, F. Şengün, Ü. Cansu, B. Başıyigit, H. Sağlam and A. Karaaslan, *Food Chem.*, 2021, **337**, 127748.
- 44 W.-C. Hsieh, C.-P. Chang and Y.-L. Gao, *Colloids Surf., B*, 2006, **53**, 209–214.
- 45 J. K. Rutz, C. D. Borges, R. C. Zambiasi, M. M. Crizel-Cardozo, L. S. Kuck and C. P. Noreña, *Food Chem.*, 2017, **220**, 59–66.
- 46 S. Songkro, P. Yapong, P. Puechpan, D. Maneenuan and P. Boonme, *Songklanakarin J. Sci. Technol.*, 2018, **40**, 767–775.
- 47 O. Vega, J. J. Araya, M. Chavarría and E. Castellón, *J. Sol-Gel Sci. Technol.*, 2016, **79**, 584–595.
- 48 H. Lee, S. Lee, I. Cheong and J. Kim, *J. Microencapsulation*, 2002, **19**, 559–569.
- 49 C. Sebaaly, A. Jrajaj, H. Fessi, C. Charcosset and H. Greige-Gerges, *Food Chem.*, 2015, **178**, 52–62.
- 50 Y. Sekita, K. Murakami, H. Yumoto, H. Mizuguchi, T. Amoh, S. Ogino, T. Matsuo, Y. Miyake, H. Fukui and Y. Kashiwada, *Biosci., Biotechnol., Biochem.*, 2016, **80**, 1205–1213.
- 51 J. F. Ayala-Zavala, H. Soto-Valdez, A. González-León, E. Álvarez-Parrilla, O. Martín-Belloso and G. A. González-Aguilar, *J. Inclusion Phenom. Macrocyclic Chem.*, 2008, **60**, 359–368.
- 52 Y. Nakai, K. Yamamoto, K. Terada, A. Kajiyama and I. Sasaki, *Chem. Pharm. Bull.*, 1986, **34**, 2178–2182.
- 53 M. Sauceau, E. Rodier and J. Fages, *J. Supercrit. Fluids*, 2008, **47**, 326–332.
- 54 K. Munhuweyi, O. J. Caleb, A. J. van Reenen and U. L. Opara, *LWT*, 2018, **87**, 413–422.
- 55 J. Wang, Y. Cao, B. Sun and C. Wang, *Food Chem.*, 2011, **127**, 1680–1685.
- 56 F. Kayaci and T. Uyar, *J. Agric. Food Chem.*, 2011, **59**, 11772–11778.
- 57 C. L. Del Toro-Sánchez, J. F. Ayala-Zavala, L. Machi, H. Santacruz, M. A. Villegas-Ochoa, E. Alvarez-Parrilla and G. A. González-Aguilar, *J. Inclusion Phenom. Macrocyclic Chem.*, 2010, **67**, 431–441.

